Different altered pattern expression of genes related to apoptosis in isolated methylmalonic aciduria type and combined with homocystinuria type

Ana Jorge-Finnigan, Alejandra Gámez, Belén Pérez, Magdalena Ugarte, Eva Richard

▶ **To cite this version:**

Ana Jorge-Finnigan, Alejandra Gámez, Belén Pérez, Magdalena Ugarte, Eva Richard. Different altered pattern expression of genes related to apoptosis in isolated methylmalonic aciduria type and combined with homocystinuria type. Biochimica et Biophysica Acta - Molecular Basis of Disease, 2010, 1802 (11), pp.959. 10.1016/j.bbadis.2010.08.002 . hal-00623301

HAL Id: hal-00623301
https://hal.science/hal-00623301

Submitted on 14 Sep 2011

HAL is a multi-disciplinary open access archive for the deposit and dissemination of scientific research documents, whether they are published or not. The documents may come from teaching and research institutions in France or abroad, or from public or private research centers.

L'archive ouverte pluridisciplinaire **HAL**, est destinée au dépôt et à la diffusion de documents scientifiques de niveau recherche, publiés ou non, émanant des établissements d'enseignement et de recherche français ou étrangers, des laboratoires publics ou privés.

Accepted Manuscript

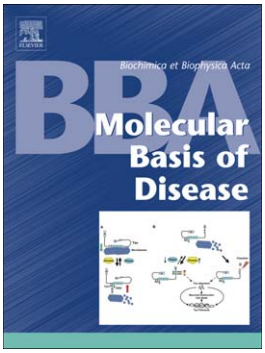

Different altered pattern expression of genes related to apoptosis in isolated methylmalonic aciduria *cblB* type and combined with homocystinuria *cblC* type

Ana Jorge-Finnigan, Alejandra Gámez, Belén Pérez, Magdalena Ugarte, Eva Richard

PII: S0925-4439(10)00164-X
DOI: doi: 10.1016/j.bbadis.2010.08.002
Reference: BBADIS 63152

To appear in: *BBA - Molecular Basis of Disease*

Received date: 8 March 2010
Revised date: 29 July 2010
Accepted date: 3 August 2010

Please cite this article as: Ana Jorge-Finnigan, Alejandra Gámez, Belén Pérez, Magdalena Ugarte, Eva Richard, Different altered pattern expression of genes related to apoptosis in isolated methylmalonic aciduria *cblB* type and combined with homocystinuria *cblC* type, *BBA - Molecular Basis of Disease* (2010), doi: 10.1016/j.bbadis.2010.08.002

This is a PDF file of an unedited manuscript that has been accepted for publication. As a service to our customers we are providing this early version of the manuscript. The manuscript will undergo copyediting, typesetting, and review of the resulting proof before it is published in its final form. Please note that during the production process errors may be discovered which could affect the content, and all legal disclaimers that apply to the journal pertain.

ACCEPTED MANUSCRIPT

Different altered pattern expression of genes related to apoptosis in isolated methylmalonic aciduria *cblB* type and combined with homocystinuria *cblC* type

Ana Jorge-Finnigan[a, 1], Alejandra Gámez[a, 1], Belén Pérez[a], Magdalena Ugarte[a,*] and Eva Richard[a].

[a]Centro de Diagnóstico de Enfermedades Moleculares, Centro de Biología Molecular "Severo Ochoa" CSIC-UAM, Departamento de Biología Molecular. Universidad Autónoma de Madrid, Centro de Investigación Biomédica en Red de Enfermedades Raras (CIBERER), Madrid, Spain.

[*]To whom correspondence should be addressed: Centro de Biología Molecular "Severo Ochoa". Laboratorio 204. C/ Nicolás Cabrera Nº 1. Universidad Autónoma de Madrid, 28049 Madrid, Spain. Phone: +34914974589. Fax: +34917347797. E-mail: mugarte@cbm.uam.es

[1]These authors contributed equally to this work.

ACCEPTED MANUSCRIPT

ACCEPTED MANUSCRIPT

ABSTRACT

An increased reactive oxygen species (ROS) production and apoptosis rate have been associated with several disorders involved in cobalamin metabolism, including isolated methylmalonic aciduria (MMA) *cblB* type and MMA combined with homocystinuria (MMAHC) *cblC* type. Given the relevance of p38 and JNK kinases in stress-response, their activation in fibroblasts from a spectrum of patients (*mut*, *cblA*, *cblB*, *cblC* and *cblE*) was analyzed revealing an increased expression of the phosphorylated-forms, specially in *cblB* and *cblC* cell lines that presented the highest ROS and apoptosis levels. To gain further insight into the molecular mechanisms responsible for the enhanced apoptotic process observed in *cblB* and *cblC* fibroblasts, we evaluated the expression pattern of 84 apoptosis-related genes by quantitative real-time PCR. An elevated number of pro-apoptotic genes was overexpressed in *cblC* cells showing a higher rate of apoptosis compared to *cblB* and control samples. Additionally, apoptosis appears to be mainly triggered through the extrinsic pathway in *cblC*, while the intrinsic pathway was primarily activated in *cblB* cells. The differences observed regarding the apoptosis rate and preferred pathway between *cblB* and *cblC* patients who both built-up methylmalonic acid, might be explained by the accumulated homocysteine in the *cblC* group. The loss of MMACHC function in *cblC* patients might be partially responsible for the oxidative stress and apoptosis processes observed in these cell lines. Our results suggest that ROS production may represent a genetic modifier of the phenotype and support the potential of using antioxidants as a novel therapeutic strategy to improve the severe neurological outcome of these rare diseases.

Keywords: Methylmalonic aciduria; homocystinuria; ROS; apoptosis; PCR array; stress-kinases.

ACCEPTED MANUSCRIPT

1. INTRODUCTION

Mitochondrial respiratory chain generates free radicals, also known as reactive oxygen species (ROS) which are produced in physiological and pathological conditions. ROS are molecules or ions with unpaired electrons (OH^- and O_2^-) which are neutralized by endogenous antioxidant defense systems that reduce their formation or promote their inactivation by the activity of several proteins, such as superoxide dismutase and catalase [1]. Reactive species are necessary for normal cell function, serving as signal molecules for important physiological roles; however when they are produced at high levels or when the antioxidant defenses are deficient, ROS may cause damage to the cells representing a fundamental mechanism of human disease [2]. In most cases, the deleterious effect of ROS is a function of intracellular cell-death activation [3]. Apoptosis is a form of cell suicide that plays an important role in development and maintenance of tissue homeostasis in multicellular organisms [4]. The apoptosis pathways can be broadly grouped into two main categories: (1) the extrinsic or receptor-mediated pathway which involves ligand-induced aggregation of death receptors resulting in the activation of pro-apoptotic caspase-8 and caspase-10; and (2) the intrinsic or mitochondrial-mediated pathway where the fate of the cell is determined at the mitochondrial membrane level by the balance between pro-apoptotic and anti-apoptotic members of the BCL-2 family [5, 6]. In humans, several lines of evidence point toward oxidative damage and defects in programmed cell death on a number of pathologies, including autoimmunity, cancer, mitochondrial and neurodegenerative diseases [7-11].

Alterations in mitochondrial function caused by inhibition of mitochondrial energy metabolism also exert a relevant role in the pathophysiology of a number of inherited metabolic disorders (IMD), such as maple syrup urine disease, propionic

ACCEPTED MANUSCRIPT

acidemia and methylmalonic aciduria (MMA) among others [12, 13]. Vitamin B_{12} (cobalamin, Cbl), in the form of the cofactors adenosylcobalamin (AdoCbl) and methylcobalamin (MeCbl), is required by the mitochondrial enzyme methylmalonyl-CoA mutase (MUT) and by the cytosolic enzyme methionine synthase (MTR), respectively. Inherited disorders of Cbl metabolism are rare conditions caused by deficiencies in MUT, MTR or methylmalonyl-CoA epimerase enzymes, or alternatively by defects in at least 6 different genes involved in Cbl adsorption, transport or cofactors´ synthesis defining different complementation groups. The *cblA* (MIM#251100), *cblB* (MIM# 251110), *cblD* variant 2 (MIM#277410) and *mut* (MIM#251000) disorders cause isolated MMA; *cblC* (MIM#277400), *cblD variant 1* (MIM#277410) and *cblF* (MIM#277380)) cause combined MMA with homocystinuria (MMAHC); and *cblE* (MIM#236270) and *cblG* (MIM#250940) cause isolated homocystinuria [14, 15]. Patients belonging to the *cblB* group present defects in the *MMAB* gene (MIM#607568) which encodes a mitochondrial enzyme member of the PduO family of cobalamin adenosyltransferases: ATP:cob(I)alamin adenosyltransferase (ATR) implicated in adenosylcobalamin (AdoCbl) metabolism [16]. The *cblC* type group is the most common genetic defect in cobalamin metabolism which is associated with defects in the *MMACHC* gene (MIM#609831), affecting both AdoCbl and MeCbl metabolism [17]. The cytosolic *MMACHC* gene product is responsible for early processing of both CNCbl (decyanation) and alkylcobalamins (dealkylation) in mammalian cells [18].

Despite continuous attempts during the last 20 years to improve therapy for these diseases, the overall outcome of MMA and MMAHC patients remains disappointing; many of them still present severe symptoms that include psychomotor retardation and long-term neurological damage [19-21]. Although three

ACCEPTED MANUSCRIPT

pathomechanisms have been proposed to explain the neurological damage (the “toxic metabolite hypothesis”, synergistic inhibition of mitochondrial energy metabolism and dicarboxylic acids and the “trapping hypothesis”) [22], the mechanisms underlying the pathophysiology of MMA and MMAHC are far from being understood. Data from our laboratory support the implication of oxidative stress in the pathophysiology of these disorders [23-25]. Fibroblasts from *cblB* and *cblC* patients showed a significant increase in intracellular ROS content. In addition, the mitochondrial oxidative stress marker, manganese superoxide dismutase (MnSOD), was overexpressed in patients’ cell lines in comparison with controls suggesting a cellular response to intrinsic ROS stress. Moreover, patients´ cells showed a higher rate of apoptosis compared to controls. Our results also indicate that this process primarily involves the mitochondrial/caspase-dependent pathway in patients with *cblB* disorder [24]. In addition to our observations, altered mitochondrial morphology and respiratory chain dysfunction have been recently described in a background-modified *mut*-knockout mouse and in the liver from a *mut* MMA patient revealing mitochondrial dysfunction and glutathione depletion [26]. Furthermore, there is supporting data from different samples, such as tissues and cellular extracts from treated laboratory animals [27-29] and urinary samples from MMA patients [12] that correlate oxidative stress with this human disease.

In support of our previous observations and given the high interest of this topic, we have investigated the activation of p38 and JNK stress kinases by immunoblotting along with the expression profiling of a set of genes relevant to the apoptosis pathways by PCR array in patients´ cells with defects in Cbl metabolism. The combination of these powerful approaches has allowed the identification of genes specifically related to the mechanisms of stress response in patients with *cblB* and *cblC* disorders contributing to elucidate the pathophysiology of these rare metabolic diseases.

ACCEPTED MANUSCRIPT

2. MATERIALS AND METHODS

2.1. Samples

Fibroblast cell lines from 19 patients were used in this study, including 2 *cblA* (P1, P2), 3 *cblB* (P3-P5*)*, 11 *cblC* (P6-P16), 1 *cblE* (P18) and 1 mut^0 (P17) patients with defects in cobalamin metabolism, and 1 individual with defects in cystathionine β-synthase (CBS) which presents homocystinuria and was used as a control (P19). None of the patients reported herein were referred from the newborn screening metabolic program; all of them were clinically diagnosed after presenting a metabolic crisis. Patients were referred from clinics to be biochemically and/or genetically diagnosed at Centro de Diagnóstico de Enfermedades Moleculares in Madrid. Relevant clinical and molecular data, as well as references about individual patients included in this study are provided in Table 1. Skin fibroblasts from five controls (GM09503, GM08333, GM08429, GM08680 and GM03348) were obtained from Coriell Cell Repositories (NJ, USA). Fibroblast cultures were established from patients´ and controls´ skin biopsies and cultivated according to standard procedures [24]. Ethical approval for the use of human samples in the study was granted by the Ethics Committee of the Universidad Autónoma de Madrid.

2.2. Expression of human *MMACHC* cDNA in fibroblast cells

Wild-type *MMACHC* cDNA was generated by RT-PCR from total RNA extracted from normal human fibroblasts and confirmed by sequencing. This cDNA product was cloned into pGEM®-T Easy vector (Promega, Madison, WI, USA), and then subcloned into a bicistronic green fluorescent protein (GFP)-expressing MIGR1-retroviral vector [30]. Retroviruses were generated by transient co-transfection with the retroviral vector, and pGagPol and VSVG plasmids using Fugene 6 (Roche Applied Science, Mannheim, Germany) in 293T/17 cells. Retroviruses encoding both GFP and

ACCEPTED MANUSCRIPT

MMACHC proteins, or GFP alone were used to infect fibroblasts from patients P6 (*cblC*), P7 (*cblC*), P4 (*cblB*) and a control cell line. The control cell line was used as an internal control of the assay. Cells were selected for GFP expression using fluorescence activating cell sorting (FACS) on a FACSCVantage SE cell sorter (BD Biosciences, San Jose, CA, USA). MMACHC activity was indirectly measured by the analysis of radioactivity incorporation from [1-^{14}C] propionate into acid-precipitable material in infected fibroblasts [31]. Propionate oxidation is catalyzed by two mitochondrial enzymes: the biotin-dependent propionyl-CoA carboxylase and the AdoCbl-dependent methylmalonyl-CoA mutase (MUT). Patients with defects in *MMAB* and *MMACHC* genes exhibit deficient propionate incorporation since their gene products are involved in AdoCbl synthesis.

2.3. RT^2 Profiler^{TM} PCR Array human apoptosis

Total RNA was isolated from fibroblasts using MagNA Pure Compact RNA Isolation kit and MagNA Pure Compact instrument (Roche Applied Science). Samples were quantitated spectrophotometrically at 260 nm using the Nanodrop ND-1000 photometer (Thermo Scientific, Wilmington, MA, USA).

Real-time PCR reactions were analyzed in total RNA using the Human Apoptosis RT^2 Profiler^{TM} PCR Array (SuperArray Bioscience Corporation, Frederick, MD, USA) according to manufacturer's protocol. Briefly, cDNA was prepared from 750 ng total RNA using RT^2 PCR array first strand kit (SuperArray Bioscience). cDNA was diluted by adding RNase-free water. The PCR was carried out using a LightCycler® 480 apparatus (Roche Applied Science). For one 96-well-plate of the PCR array, 2550 µl of PCR master mix containing 2x SuperArray RT^2 qPCR Master Mix and 102 µl of diluted cDNA was prepared, and aliquots of 25 µl were added to each well. Universal

ACCEPTED MANUSCRIPT

cycling conditions (10 min at 95ºC, 15 s at 95ºC, 1 min 60ºC for 40 cycles) were applied.

The human Apoptosis RT^2 Profiler PCR Array profiles the expression of 84 key genes involved in apoptosis or programmed cell death. The array includes the TNF ligands and their receptors; members of the BCL-2, caspase, IAP, TRAF, CARD, death domain, death effector domain, and CIDE families; as well as genes involved in the p53 and ATM pathways (http://www.sabiosciences.com/rt_pcr_product/HTML/PAHS-012A.html).

2.4. Data normalization and analysis

Several patients´ fibroblasts from *cblB* and *cblC* complementation groups were used to perform the PCR array. *cblB* group comprises patients number 4 and 5 (pool of *cblB* patients), *cblC* group includes patients 6, 7, 9, 12, 13 and 15 (pool of *cblC* patients); and control group includes GM08429, GM08680, GM03348 and GM09503 (pool of controls). Five endogenous control genes, beta-2-microglobulin (B2M), hypoxanthine phosphoribosyltransferase 1 (HPRT1), ribosomal protein L13a (RPL13A, glyceraldehyde-3-phosphate dehydrogenase (GAPDH) and β-actin (ACTB), present on the PCR array were used for normalization. Relative quantification of apoptotic gene expression was analyzed by the comparative threshold cycle (Ct) method [32, 33]. C_T was defined as 35 for the ΔC_T calculation when the signal was below detectable limits. ΔC_T was calculated as the difference in C_T between the target gene and the average of housekeeping genes for each sample. Then, the average of the ΔC_T of the *cblB* patients´cell lines was calculated and named ΔC_T (pool of *cblB* patients), the same formula was applied to the *cblC* cell lines and to the control cell lines that were called ΔC_T (pool of *cblC* patients) and ΔC_T (pool of controls), respectively. The following formula was applied to calculate the relative amount of transcripts in patients´ groups

ACCEPTED MANUSCRIPT

respect to controls: $\Delta\Delta C_T$ (*cblB*) = ΔC_T (pool of *cblB* patients) - ΔC_T (pool of controls) for each gene; and $\Delta\Delta C_T$ (*cblC*) = ΔC_T (pool of *cblC* patients) - ΔC_T (pool of controls) for each gene. The fold-change for each gene in both groups of patients relative to the control group was calculated as $2^{-\Delta\Delta CT}$. Changes in gene expression between patients and controls were illustrated as a fold-increase/decrease. Using cut-off criteria, a 1.5-fold induction or a 0.6-fold repression of gene expression were considered to be of biological relevance. Results are represented as *cblB*-fold change and *cblC*-fold-change in Table 2.

For the infected P6 (*cblC*), P7 (*cblC*) and P4 (*cblB*) patients´fibroblasts, $\Delta\Delta C_T$ was calculated as ΔC_T (of each cell line expressing GFP-MMACHC) - ΔC_T (of each cell line expressing GFP). The fold-change for each gene in P6, P7 and P4 expressing GFP-MMACHC relative to the same cell line expressing GFP was calculated as $2^{-\Delta\Delta CT}$.

2.5. Western Blot analysis

A total of 4 x 10^5 fibroblast cells of each line were placed in 6-well plates 24 h prior protein analysis. Cells were lysated with 50 µl/well of ice-cold lysis buffer (1% Triton X-100, 10% glycerol, 150 mM NaCl, 10 mM Tris-HCl pH 7.5, protease inhibitor cocktail tables (Roche Applied Science), 10mM sodium fluoride, 1mM sodium pyrophosphate, 1mM sodium orthovanadate and 1 mM DTT). After centrifugation, protein content from supernatants was determined by Bradford method (Bio-Rad Laboratories, Hercules, CA, USA) using BSA as standard. Samples were loaded onto 10% or 4-12% NuPAGE Novex Bis-Tris mini gels (Invitrogen, Carlsbad, CA, USA) and blotted onto nitrocellulose membranes using iBlot Dry Blotting system (Invitrogen). Poinceau staining was used to verify equal amounts of protein loads. Western blotting was carried out using phospho-p38 MAP kinase (Thr180/Tyr182) polyclonal antibody (Cell Signaling Technology, Inc, Danvers, MA, USA), p38 polyclonal antibody (Santa

ACCEPTED MANUSCRIPT

Cruz Biotechnology, Inc, Santa Cruz, CA, USA), phospho-SAPK/JNK (Thr183/Tyr185) polyclonal antibody (Cell Signaling Technology, Inc), JNK2 polyclonal antibody (Cell Signaling Technology, Inc), BCL-2 mouse monoclonal antibody (Santa Cruz Biotechnology, Inc) and NOL-3 polyclonal antibody (Santa Cruz Biotechnology, Inc). Secondary antibodies were used as IgG-horseradish peroxidase conjugated and were detected by the Enhanced Chemiluminescence System (GE Healthcare, Berkshire, UK). Protein quantification was performed using a calibrated densitometer GS-800 (Bio-Rad Laboratories).

2.6. Apoptosis studies

Assays were performed when cultures reached 75-85% of confluence. Controls and patients´ fibroblast cell lines (P4, P5, P6, P7, P9, P12, P13 and P15) ranged between 7 and 10 passages. The cultures were treated with different stimulus (all of them from Sigma-Aldrich, St Louis, MO): i) 2 µM staurosporine for 1 h; ii) 20 ng/ml TNF-α and 25 µg/ml cycloheximide (CHX) for 20 h; and iii) 20 mM Tiron® (4,5-Dihydroxy-1,3-benzenedisulfonic acid disodium salt) for 20 h. Apoptotic cells were identified and quantitated by flow cytometry using the annexin V-DY634 apoptosis detection kit (Immunostep Research, Salamanca, Spain) as previously described in [25].

ACCEPTED MANUSCRIPT

3. RESULTS

3.1. p38 MAPK/JNK stress signaling pathway

ROS can activate several signaling pathways in cells including those that regulate cell death. One goal of this work was to analyze the activation of two proteins belonging to the mitogen-activated protein kinase (MAPK) superfamily, p38 kinase and Jun N-terminal kinase (JNK), to compare their activation with the ROS levels previously detected in MMA patients [24, 25]. We have analyzed the expression of the activated forms of p38 and JNK proteins by immunoblotting in a spectrum of patients´ cell lines with defects in Cbl metabolism belonging to different complementation groups (*mut, cblA, cblB, cblC and cblE*) and in a patient's cell line with defects in CBS (Table 1). The expression pattern of phosphorylated p38 and JNK proteins was individually normalized by the protein expression of total p38 and total JNK proteins which include both the phosphorylated and non-phosphorylated forms. Thus, an increased expression of phospho-p38 has been detected in the patients´ cell lines which had the highest ROS levels: *cblB* (P4) (Fig. 1A), *cblC* (P7, P9, P12, P15 and P13) (Fig. 1A), *cblE* (P18) (Fig. 1B) and the cell line with defects in CBS (P19) (Fig. 1B). Phospho-JNK was overexpressed in *cblB* fibroblasts (P4 and P5) (Fig. 1A and 1B) as well as in *cblC* cell lines (P7, P9, P12, P15 and P13) (Fig. 1A) with the highest ROS levels. A group of *cblC* cell lines which presented the lowest ROS content, also showed the lowest activation of these kinases (P14, P6, P10, P8, P11, P16) (Fig. 1C). Quantitative densitometric analysis demonstrated a 1.5-2.5-fold higher expression for phospho-p38 and a 1.5-1.8-fold higher expression for phospho-JNK in half of the patients´ cell lines compared to controls (Supplementary Fig. 1). The results obtained from the p38 protein activation correlated to the ROS levels previously observed in 16 of the 19 cell lines (Pearson's correlation coefficient, $r = 0.72$); however there was not a

ACCEPTED MANUSCRIPT

significant correlation between p-JNK expression and ROS levels probably due to the lower activation of JNK compared to p38 which is particularly highly activated.

Given the biochemical response to hydroxocobalamin (OHCbl) *in vivo* in *cblC* and in some *cblB* affected-patients and/or *in vitro* in patients´ cell lines [25, 34, 35], and the decrease in ROS levels in OHCbl-treated cells [25], the expression pattern of stress-kinases was studied in depth for two *cblC* patients (P6, P7), one *cblB* patient and a control cell line supplemented with 1 µg/ml of OHCbl during 72 h. P6 and P7 cell lines were selected from the *cblC* group because even when they share the same genotype they present a different kinases´ activation response. P-p38 expression was significantly reduced in P7 (35%), and slightly reduced in P6 (17%) and P4 (18%) fibroblasts after OHCbl treatment compared to each cell line no-treated (data not shown). In the case of p-JNK expression, all the three cell lines presented a moderate reduction (P6: 27%, P7: 25% and P4: 31%). Stress-kinases activation is overall reduced in P7 cell line, which presented high ROS and apoptosis rate. There was no reduction in both kinases´expression in the control cell line after OHCbl treatment. This moderate decrease in the activation of these stress-kinases is in accordance with our previous studies that shown a moderate decrease of relative ROS levels (range 10-20%) after OHCbl cell incubation [25].

3.2. Human apoptosis PCR array

In order to deepen the understanding of the apoptosis process in these groups of disorders with defects in Cbl metabolism, we performed a PCR array designed to determine the expression profile of a group of 84 genes, including TNF ligands and their receptors, members of the BCL-2, caspase, IAP, TRAF, CARD, death domain, death effector domain, CIDE families, p53 and DNA damage response, all of which are involved in apoptosis. In this array, we have included four controls, two patients

ACCEPTED MANUSCRIPT

belonging to the *cblB* group (P4 and P5) with isolated MMA and six *cblC* patients (P6, P7, P9, P12, P13, P15) with MMAHC that previously showed the highest ROS content and also a high rate of apoptosis, as mentioned above.

In order to understand the implication of each gene in the apoptosis mechanisms, we classified the genes with altered expression in two groups: i) pro-apoptotic genes and ii) anti-apoptotic genes. We identified the altered expression of 30 genes in *cblB* and 37 genes in *cblC* cell lines (Table 2). In *cblB* patients, 20 pro-apoptotic genes (9 overexpressed and 11 under-expressed), and 10 antiapoptotic genes (4 overexpressed and 6 under-expressed) were detected (Table 3). In the group of *cblC* patients, 21 pro-apoptotic genes (18 overexpressed and 3 under-expressed), and 16 antiapoptotic genes (15 overexpressed and 1 under-expressed) were identified (Table 3). The fold-change of the expression pattern was moderate; only 11 genes showed a fold-change rate higher than 2. The highest overexpression, among all the genes studied in both *cblB* and *cblC* cell lines, was the activator of apoptosis harakiri (HRK).

When comparing the relative gene expression between *cblB* and *cblC* groups, several differences were observed. *CblC* cell lines presented a higher number (18 versus 9) and a higher fold-change (2-2.5-fold versus 1.5-1.8-fold) of overexpressed pro-apoptotic genes than *cblB* cell lines (Supplementary Table 1). Most of the pro-apoptotic genes with an increased expression in *cblC* fibroblasts belong to different families, such as TNF ligand and receptor families and CASP10 among others (Table 2), which are involved in the extrinsic or the death receptor-mediated apoptosis pathway. In contrast, these genes were under-expressed in *cblB* lines (Table 3). In addition, among the overexpressed pro-apoptotic genes in *cblB* cell lines, CASP9 and HRK genes (Table 2) are involved in the intrinsic or mitochondrial apoptosis pathway.

ACCEPTED MANUSCRIPT

In order to confirm the gene expression pattern observed, a subset of genes was selected (BCL-2 and NOL-3, the transcripts that showed the highest expression among the anti-apoptotic-related genes) to determine their protein expression pattern in two *cblB* (P3 and P4) and in five *cblC* patients´ cells (P7, P9, P12, P13 and P15) by immunoblotting (Supplementary Fig. 2). Differential protein expression was consistent with the array results confirming that NOL-3 and BCL-2 are specially increased in *cblC* cell lines. NOL-3 protein expression appears particularly increased in *cblC* fibroblasts from P7, P9, P15 and P13 patients (1.5-2-fold) (Supplementary Fig. 2A). Finally, overexpression of BCL-2 was specially detected in the *cblC* cell lines: P9, P12, P15 and P13 (2-4 fold-change) (Supplementary Fig. 2B).

To verify if the MMACHC loss of function is related to the observed apoptosis process, we analyzed the expression pattern of the previously studied apoptotic genes in the same patients´ fibroblasts that were selected for OHCbl study, two from the *cblC* group (P6, P7) and one from the *cblB* one (P4), and in a control cell line, all of them infected with wild-type *MMACHC* cDNA using a retroviral vector. Function of MUT, measured by the incorporation of label from [^{14}C]-propionate into cellular macromolecules, was restored to nearly the low range of control levels in infected *cblC* fibroblasts: 85% and 51% in P6 and P7, respectively. The radioactivity incorporation was similar in the non-infected control cell line compared to the infected line expressing MMACHC-GFP proteins and also GFP alone reflecting no substantial change in the metabolic pathway. The MUT function was not restored in *cblB* fibroblasts (P4) due to the intrinsic *MMAB* gene defect. Initially, in order to select which genes were up-regulated in the non-infected cell lines, we performed an individually fold-change comparison for each gene in the non-infected P6, P7 and P4 cells respect to the non-infected pool of control individuals. A total of 49 different genes were up-regulated and

ACCEPTED MANUSCRIPT

then selected for the analysis of the MMACHC expression effect in these cell lines which shared some of these genes: 15 genes were up-regulated in P6, 40 in P7 and 13 in P4. The gene expression response to retroviral infection in patients´ cell lines expressing MMACHC protein is shown in Table 4. The fold-change for each gene was calculated in each cell line expressing MMACHC protein respect to the same cell line expressing GFP alone; then the genes were selected based on the criteria of a 1.5-fold induction or a 0.65-fold repression. The global result obtained in the three cell lines showed that 27 genes were down-regulated, 3 were undetectable and 19 did not show any change in their expression of the total of 49 genes that were previously up-regulated. No essential changes were detected in relation to the genes that were down-regulated in the non-infected cell lines and the genes that were up-regulated post-infection (19 genes versus 2).

Interestingly, P7 (*cblC*) which showed a high activation of stress-kinases and apoptosis rate in non-infected cells, presented the highest number of down-regulated genes (19) along with the highest fold-change in gene repression when MMACHC protein was expressed in this patient's cell line. It is worth noting that the most relevant genes previously up-regulated in non-infected *cblB* and *cblC* groups (TNF ligand, TNF receptor, Bcl-2, caspase, CARD and CIDE families) indicated in Table 2, were down-regulated in *cblC* fibroblasts (P6 and P7) expressing MMACHC by retroviral infection (Table 4). Taking into account the functional gene groupings, 19 genes down-regulated were pro-apoptotic genes. In summary, 55% of the array gene expression (27 genes down-regulated out of 49 total genes selected) has been corrected when MMACHC function was partially restored.

3.3. Functional studies of cell death in response to different stimulus that activate apoptosis pathways, and in response to ROS scavenger

ACCEPTED MANUSCRIPT

To further investigate the activation of the extrinsic and intrinsic apoptosis pathways in the different cell lines analyzed by PCR array, fibroblasts were cultured in presence of different stimulus, such as staurosporine and TNF-α (Fig. 2). Staurosporine, an activator of the intrinsic mitochondrial pathway [36], induced apoptosis in all the studied cell lines (>2-fold) (Fig. 2A), specially in *cblB* patients (P5 and P4) (≥ 3-fold) and in those *cblC* patients (~3-fold) which previously presented the highest ROS and apoptosis levels [25]. On the other hand, the extrinsic apoptosis pathway was induced using TNF-α/CHX in a great extent in the *cblC* cell lines (2-3-fold) (Fig. 2B). To establish a link between ROS production and the cell death execution, the effects of an antioxidant were studied. Tiron®, a scavenger of superoxide anion, is able to quench ROS production (data not shown) and cell death (Fig. 2C). The percentage of apoptotic cells were significantly reduced (~50%) overall in P4 (*cblB*), P7 (*cblC*) and P13 (*cblC*) cell lines which presented the highest ROS and apoptosis levels.

ACCE

ACCEPTED MANUSCRIPT

4. DISCUSSION

ROS play an important role in the regulation of cellular mechanisms leading to the activation of essential signaling proteins, such as p38 and JNK which belong to the mitogen-activated protein kinases (MAPKs) family [37]. Activation of these signaling pathways has been suggested to mediate neuronal apoptosis in Alzheimer's disease, Parkinson disease and amyotrophic lateral sclerosis [38]. One of the main goals of this work was to study the activation of p38 and JNK kinases which revealed a stimulation of these activated stress-sensing pathways, specially in those patients that presented higher levels of intracellular ROS (*cblB, cblC, cblE* and *CBS*-deficient patient). The fact that fibroblasts from *cblC* patients with MMAHC, *cblE* with homocystinuria and the CBS deficient patient with homocystinuria present the highest ROS level [25] and phospho-p38 activation, suggests that homocysteine might play a relevant role in stress-response, as it is indicated below. Mitochondria are influenced by pro-apoptotic signal transduction through the JNK pathway [39], a higher expression of phosphorylated JNK protein in *cblB* cell lines compared to the other groups and control cell lines suggests that the intrinsic or mitochondrial pathway is its preferred apoptosis path. These promising results will be followed up with further studies focused on upstream components of the signaling pathways that culminate in the activation of p38 and JNK proteins due to these metabolic disorders.

In order to confirm the differences observed regarding the apoptosis process in both *cblB* and *cblC* cell lines, we performed a PCR array designed to determine the expression profile of a group of apoptotic genes. Our results provide clear evidence that *cblB* and *cblC* cell lines do not share a common apoptotic pathway given the low degree of similarity in their apoptotic gene expression. In *cblC* patients´ fibroblasts, the induction of apoptosis has been essentially maintained by the activation of the death

ACCEPTED MANUSCRIPT

receptor-mediated apoptotic pathway. These cell lines showed a highly up-regulation of components of the extrinsic pathway, the majority of them belong to the TNF ligand (LTA, TNF, TNFSF10) and receptor families (TNFRSF5, TNFRSF1A, TNFRSF25, TNFRSF10A, TNFRSF21, CD27, TNFRSF9, LTBR) and CASP10. In contrast, most of these genes were down-regulated in *cblB* patients´ fibroblasts. On the other hand, the up-regulation of CASP9 has been mainly observed in fibroblasts from patients with *cblB* disorder, as we previously observed by flow cytometry [24]. CASP 9 activation along with the induction of phosphorylated JNK kinase suggest the involvement of the mitochondrial pathway overall in the *cblB* group. The overexpression of additional genes has also been detected in both *cblB* and *cblC* patients´ fibroblasts, including HRK, MCL1, BCL2A1 and NOL3 which interact with the intrinsic or mitochondrial pathway. Additionally, the differences observed regarding the preferred apoptosis pathway between *cblB* and *cblC* patients were further confirmed using different apoptosis stimulus. Therefore, *cblB* patients´ cell lines presented a higher rate of apoptosis compared to the other cell lines when all were treated with staurosporine, showing a higher sensitivity to this death activator of the intrinsic or mitochondrial pathway. The relative contribution of mitochondrial oxidative phosphorylation to the supply of metabolic energy in the cell could be responsible for the different cell death response to staurosporine between different cell lines [40]. However, TNF-α induced a higher apoptosis rate in *cblC* cell lines which possibly are more sensitive to the extrinsic pathway activation.

Cell lines from patients with *cblC* disorder present a gene expression profiling that suggests a higher rate of apoptosis compared to *cblB* fibroblasts. Among the pro-apoptotic genes with altered expression, 9 were overexpressed in the *cblB* group versus 18 in the *cblC* one, and 11 were under-expressed in the *cblB* group versus 3 in *cblC*.

ACCEPTED MANUSCRIPT

Our findings are consistent with our previous studies in which *cblC* patients´ fibroblasts showed the highest ROS content and the highest percentage of apoptotic cells compared to the other patients´ (*mut*, *cblA* and *cblB*) and controls´ cell lines [24, 25]. Moreover, *cblC* patients were also characterized by a higher expression of pro-apoptotic proteins of the BCL-2 family (HRK, BIK, BAX) and CIDE domain family (CIDEA, CIDEB), and by significant levels of anti-apoptotic proteins of BCL-2, IAP and TRAF families. The increased rate of apoptosis in *cblC* patients´ fibroblasts and their pattern of gene expression dominated by pro-apoptotic members might up-regulate the anti-apoptotic molecules through a compensatory response. In addition, our results proved that CASP3 was down-regulated in both patients´ groups, specially in *cblC* patients. The expression pattern of this gene might be due to an alternative regulation mechanism; however the amount of protein in these cell lines may be sufficient to trigger its activation, as we have previously observed [24].

Two pro-apoptotic genes which are members of the p53 family (TP53 and TP53BP2) were under-expressed in both *cblB* and *cblC* patients´ fibroblasts. Regulation of p53 function is highly complex and occurs at different levels. The tumour suppressor p53 can induce apoptosis through both the two main apoptotic pathways activating the transcription of genes that promote this process. Our results indicate that apoptosis observed in *cblB* and *cblC* cell lines may not be p53-dependent given that those genes were down-regulated. It is also interesting to note that p53 can modulate the balance between glycolytic and respiratory pathways through the actions of various proteins [41], and that cells that lack functional p53 show an enhanced glycolysis activity and lower oxygen consumption by mitochondrial respiration [42]. Likewise, we propose that in *cblB* and *cblC* patients the flux through the glycolytic pathway may be increased due to a mitochondrial dysfunction, as it has been described in Huntington´s disease, a

ACCEPTED MANUSCRIPT

progressive neurodegenerative disorder [43], and in cancer [44]. In order to test this hypothesis, complementary studies are planned to be performed.

OHCbl treatment provokes a reduction in ROS levels [25] and also in stress-kinases activation in patients´cell lines. In addition, the mRNA apoptotic expression has been ameliorated when MMACHC function was partially restored in retroviral infected patients´ fibroblasts. Our results suggest that the MMACHC defect in *cblC* patients is at least in part responsible for the increased ROS and apoptosis levels observed in these patients´ cell lines. It is important to note that there is a weak correlation between genotype and ROS and apoptosis phenotype given the variability of these levels among cell lines carrying the same mutations. This fact could be explained by other unidentified regulatory, genetic and/or epigenetic factors [45, 46], such as unlinked genes that could be involved in the OHCbl response and/or in other processes related to oxidative stress and apoptosis that can act as external modulators.

Since both *cblB* patients with isolated MMA and *cblC* with MMAHC accumulate methylmalonic acid, the built-up of homocysteine in *cblC* patients could be responsible for the differences observed in the apoptosis process in both groups of patients. In addition, the fact that ROS levels and p38 activation were also elevated in *cblE* and CBS cell lines with homocystinuria support this hypothesis. Apoptosis may be enhanced in these groups of patients by the presence of homocysteine, as it has been described in brain endothelial cells [47, 48], osteoblasts and vascular endothelial cells [49, 50]. Further analysis will provide a deeper insight into the effect of homocysteine in the activation of apoptosis and/or ROS production, as well as on the association of apoptosis with the irreversible neurological damage characteristic of these patients, which persists and in some cases can be even fatal despite the treatment [25, 51-53]. Based on the evidence from stress oxidative studies in other human diseases, it might be

ACCEPTED MANUSCRIPT

predicted that antioxidants may be a good therapeutic option. We were able to prevent the apoptosis activation *in vitro* using Tiron®, suggesting that the generation of superoxide contributes critically to the basal apoptosis levels in the cell lines studied. Further studies using other antioxidants will allow to establish the effectiveness of these compounds in the overall improvement of the patients´ health status.

5. CONCLUSIONS

In summary, we provide the first evidence that p38 and JNK MAPK pathways are activated in patients´ cell lines with defects in cobalamin metabolism, and we also demonstrate that there is a different pattern of apoptotic gene expression between *cblB* and *cblC* cells. Moreover, all the data reported herein support our previous observations in *cblC* cell lines that present the highest rate of apoptosis, and that the intrinsic or mitochondrial apoptosis pathway is activated in *cblB* fibroblasts. These observed differences could be explained by the toxic built-up of homocysteine in *cblC*, since methylmalonic acid is accumulated in both groups of patients. Therefore, the loss of MMACHC function in *cblC* patients might be partially responsible for the oxidative stress and apoptosis processes observed in these cell lines. These studies may have clinical impact because they support the potential of diminishing intracellular ROS and oxidative-stress-induced apoptosis as a novel strategy for the treatment of these devastating diseases. Eventually, patients diagnosed by the neonatal screening could benefit greatly from this new therapeutic approach.

ACCEPTED MANUSCRIPT

ACKNOWLEDGEMENTS

This work was supported by grants from Ministerio de Educación y Ciencia (SAF2007-61364) and from Fondo de Investigaciones Sanitarias (PI060512). A. Jorge-Finnigan was funded by Fondo de Investigaciones Sanitarias. A. Gámez was supported by a research contract from "Ramón y Cajal" program by Ministerio de Ciencia e Innovación. We thank A. Sánchez for her excellent technical assistance in cell culture, R. Ramos for the analysis of the array data and A. Echarri for his expert assistance in the retroviral production and infection of the cell lines. The institutional grant from Fundación Ramón Areces to the Centro de Biología Molecular "Severo Ochoa" is gratefully acknowledged.

ACCEPTED M

ACCEPTED MANUSCRIPT

REFERENCES

[1] B. Halliwell, M. Whiteman, Measuring reactive species and oxidative damage in vivo and in cell culture: how should you do it and what do the results mean?, Br J Pharmacol 142 (2004) 231-255.

[2] B. Halliwell, Free radicals, antioxidants, and human disease: curiosity cause or consequence?, Lancet 344 (1994) 721-724.

[3] M. Le Bras, M.V. Clement, S. Pervaiz, C. Brenner, Reactive oxygen species and the mitochondrial signaling pathway of cell death, Histol Histopathol 20 (2005) 205-219.

[4] N. Shivapurkar, J. Reddy, P.M. Chaudhary, A.F. Gazdar, Apoptosis and lung cancer: a review, J Cell Biochem 88 (2003) 885-898.

[5] M.O. Hengartner, The biochemistry of apoptosis, Nature 407 (2000) 770-776.

[6] H. Zhang, Q. Xu, S. Krajewski, M. Krajewska, Z. Xie, S. Fuess, S. Kitada, K. Pawlowski, A. Godzik, J.C. Reed, BAR: An apoptosis regulator at the intersection of caspases and Bcl-2 family proteins, Proc Natl Acad Sci U S A 97 (2000) 2597-2602.

[7] J.K. Andersen, Oxidative stress in neurodegeneration: cause or consequence?, Nat Med 10 Suppl (2004) S18-25.

[8] E. Trushina, C.T. McMurray, Oxidative stress and mitochondrial dysfunction in neurodegenerative diseases, Neuroscience 145 (2007) 1233-1248.

[9] S. DiMauro, E.A. Schon, Mitochondrial disorders in the nervous system, Annu Rev Neurosci 31 (2008) 91-123.

[10] K.P. Loh, S.H. Huang, R. De Silva, B.K. Tan, Y.Z. Zhu, Oxidative stress: apoptosis in neuronal injury, Curr Alzheimer Res 3 (2006) 327-337.

ACCEPTED MANUSCRIPT

[11] M.F. Beal, Mitochondria take center stage in aging and neurodegeneration, Ann Neurol 58 (2005) 495-505.

[12] P.J. Mc Guire, A. Parikh, G.A. Diaz, Profiling of oxidative stress in patients with inborn errors of metabolism, Mol Genet Metab 98 (2009) 173-180.

[13] K.R. Atkuri, T.M. Cowan, T. Kwan, A. Ng, L.A. Herzenberg, L.A. Herzenberg, G.M. Enns, Inherited disorders affecting mitochondrial function are associated with glutathione deficiency and hypocitrullinemia, Proc Natl Acad Sci U S A 106 (2009) 3941-3945.

[14] W.A. Fenton, R.A. Gravel, L.E. Rosenberg, Disorders of propionate and methylmalonate metabolism, in: C.R. Scriver, A.L. Beaudet, W. Sly, D. Valle (Eds.), The Metabolic and Molecular Bases of Inherited Disease, McGraw-Hill, New York, 2001, pp. 2165-2190.

[15] B. Fowler, J.V. Leonard, M.R. Baumgartner, Causes of and diagnostic approach to methylmalonic acidurias, J Inherit Metab Dis 31 (2008) 350-360.

[16] C.M. Dobson, T. Wai, D. Leclerc, H. Kadir, M. Narang, J.P. Lerner-Ellis, T.J. Hudson, D.S. Rosenblatt, R.A. Gravel, Identification of the gene responsible for the cblB complementation group of vitamin B12-dependent methylmalonic aciduria, Hum Mol Genet 11 (2002) 3361-3369.

[17] J.P. Lerner-Ellis, J.C. Tirone, P.D. Pawelek, C. Dore, J.L. Atkinson, D. Watkins, C.F. Morel, T.M. Fujiwara, E. Moras, A.R. Hosack, G.V. Dunbar, H. Antonicka, V. Forgetta, C.M. Dobson, D. Leclerc, R.A. Gravel, E.A. Shoubridge, J.W. Coulton, P. Lepage, J.M. Rommens, K. Morgan, D.S. Rosenblatt, Identification of the gene responsible for methylmalonic aciduria and homocystinuria, cblC type, Nat Genet 38 (2006) 93-100.

ACCEPTED MANUSCRIPT

[18] L. Hannibal, J. Kim, N.E. Brasch, S. Wang, D.S. Rosenblatt, R. Banerjee, D.W. Jacobsen, Processing of alkylcobalamins in mammalian cells: A role for the MMACHC (cblC) gene product, Mol Genet Metab 97 (2009) 260-266.

[19] C. Dionisi-Vici, F. Deodato, W. Roschinger, W. Rhead, B. Wilcken, 'Classical' organic acidurias, propionic aciduria, methylmalonic aciduria and isovaleric aciduria: long-term outcome and effects of expanded newborn screening using tandem mass spectrometry, J Inherit Metab Dis 29 (2006) 383-389.

[20] F. Horster, S.F. Garbade, T. Zwickler, H.I. Aydin, O.A. Bodamer, A.B. Burlina, A.M. Das, J.B. De Klerk, C. Dionisi-Vici, S. Geb, G. Gokcay, N. Guffon, E.M. Maier, E. Morava, J.H. Walter, B. Schwahn, F.A. Wijburg, M. Lindner, S. Grunewald, M.R. Baumgartner, S. Kolker, Prediction of outcome in isolated methylmalonic acidurias: combined use of clinical and biochemical parameters, J Inherit Metab Dis 32 (2009) 630-639.

[21] S. Kolker, J.G. Okun, Methylmalonic acid--an endogenous toxin?, Cell Mol Life Sci 62 (2005) 621-624.

[22] D. Ballhausen, L. Mittaz, O. Boulat, L. Bonafe, O. Braissant, Evidence for catabolic pathway of propionate metabolism in CNS: expression pattern of methylmalonyl-CoA mutase and propionyl-CoA carboxylase alpha-subunit in developing and adult rat brain, Neuroscience 164 (2009) 578-587.

[23] E. Richard, L. Monteoliva, S. Juarez, B. Perez, L.R. Desviat, M. Ugarte, J.P. Albar, Quantitative analysis of mitochondrial protein expression in methylmalonic acidemia by two-dimensional difference gel electrophoresis, J Proteome Res 5 (2006) 1602-1610.

[24] E. Richard, A. Alvarez-Barrientos, B. Perez, L.R. Desviat, M. Ugarte, Methylmalonic acidaemia leads to increased production of reactive oxygen

ACCEPTED MANUSCRIPT

species and induction of apoptosis through the mitochondrial/caspase pathway, J Pathol 213 (2007) 453-461.

[25] E. Richard, A. Jorge-Finnigan, J. Garcia-Villoria, B. Merinero, L.R. Desviat, L. Gort, P. Briones, F. Leal, C. Perez-Cerda, A. Ribes, M. Ugarte, B. Perez, Genetic and cellular studies of oxidative stress in methylmalonic aciduria (MMA) cobalamin deficiency type C (cblC) with homocystinuria (MMACHC), Hum Mutat 30 (2009) 1558-1566.

[26] R.J. Chandler, P.M. Zerfas, S. Shanske, J. Sloan, V. Hoffmann, S. DiMauro, C.P. Venditti, Mitochondrial dysfunction in mut methylmalonic acidemia, FASEB J 23 (2009) 1252-1261.

[27] F.U. Fontella, V. Pulrolnik, E. Gassen, C.M. Wannmacher, A.B. Klein, M. Wajner, C.S. Dutra-Filho, Propionic and L-methylmalonic acids induce oxidative stress in brain of young rats, Neuroreport 11 (2000) 541-544.

[28] L.F. Pettenuzzo, P.F. Schuck, A.T. Wyse, C.M. Wannmacher, C.S. Dutra-Filho, C.A. Netto, M. Wajner, Ascorbic acid prevents water maze behavioral deficits caused by early postnatal methylmalonic acid administration in the rat, Brain Res 976 (2003) 234-242.

[29] L.F. Pettenuzzo, C. Ferreira Gda, A.L. Schmidt, C.S. Dutra-Filho, A.T. Wyse, M. Wajner, Differential inhibitory effects of methylmalonic acid on respiratory chain complex activities in rat tissues, Int J Dev Neurosci 24 (2006) 45-52.

[30] R.C. Quackenbush, G.W. Reuther, J.P. Miller, K.D. Courtney, W.S. Pear, A.M. Pendergast, Analysis of the biologic properties of p230 Bcr-Abl reveals unique and overlapping properties with the oncogenic p185 and p210 Bcr-Abl tyrosine kinases, Blood 95 (2000) 2913-2921.

ACCEPTED MANUSCRIPT

[31] C. Perez-Cerda, B. Merinero, P. Sanz, A. Jimenez, M.J. Garcia, A. Urbon, J. Diaz Recasens, C. Ramos, C. Ayuso, M. Ugarte, Successful first trimester diagnosis in a pregnancy at risk for propionic acidaemia, J Inherit Metab Dis 12 Suppl 2 (1989) 274-276.

[32] K.J. Livak, T.D. Schmittgen, Analysis of relative gene expression data using real-time quantitative PCR and the 2(-Delta Delta C(T)) Method, Methods 25 (2001) 402-408.

[33] T.D. Schmittgen, K.J. Livak, Analyzing real-time PCR data by the comparative C(T) method, Nat Protoc 3 (2008) 1101-1108.

[34] D.S. Rosenblatt, A.L. Aspler, M.I. Shevell, B.A. Pletcher, W.A. Fenton, M.R. Seashore, Clinical heterogeneity and prognosis in combined methylmalonic aciduria and homocystinuria (cblC), J Inherit Metab Dis 20 (1997) 528-538.

[35] A. Jorge-Finnigan, C. Aguado, R. Sanchez-Alcudia, D. Abia, E. Richard, B. Merinero, A. Gamez, R. Banerjee, L.R. Desviat, M. Ugarte, B. Perez, Functional and structural analysis of five mutations identified in methylmalonic aciduria cbIB type, Hum Mutat (2010) in press.

[36] M. Nicolier, A.Z. Decrion-Barthod, S. Launay, J.L. Pretet, C. Mougin, Spatiotemporal activation of caspase-dependent and -independent pathways in staurosporine-induced apoptosis of p53wt and p53mt human cervical carcinoma cells, Biol Cell 101 (2009) 455-467.

[37] V. Temkin, M. Karin, From death receptor to reactive oxygen species and c-Jun N-terminal protein kinase: the receptor-interacting protein 1 odyssey, Immunol Rev 220 (2007) 8-21.

[38] E.K. Kim, E.J. Choi, Pathological roles of MAPK signaling pathways in human diseases, Biochim Biophys Acta 1802 (2010) 396-405.

ACCEPTED MANUSCRIPT

[39] W. Qu, H. Ke, J. Pi, D. Broderick, J.E. French, M.M. Webber, M.P. Waalkes, Acquisition of apoptotic resistance in cadmium-transformed human prostate epithelial cells: Bcl-2 overexpression blocks the activation of JNK signal transduction pathway, Environ Health Perspect 115 (2007) 1094-1100.

[40] G. Santamaria, M. Martinez-Diez, I. Fabregat, J.M. Cuezva, Efficient execution of cell death in non-glycolytic cells requires the generation of ROS controlled by the activity of mitochondrial H+-ATP synthase, Carcinogenesis 27 (2006) 925-935.

[41] T. Ide, L. Brown-Endres, K. Chu, P.P. Ongusaha, T. Ohtsuka, W.S. El-Deiry, S.A. Aaronson, S.W. Lee, GAMT, a p53-inducible modulator of apoptosis, is critical for the adaptive response to nutrient stress, Mol Cell 36 (2009) 379-392.

[42] M.G. Vander Heiden, L.C. Cantley, C.B. Thompson, Understanding the Warburg effect: the metabolic requirements of cell proliferation, Science 324 (2009) 1029-1033.

[43] J. Olah, P. Klivenyi, G. Gardian, L. Vecsei, F. Orosz, G.G. Kovacs, H.V. Westerhoff, J. Ovadi, Increased glucose metabolism and ATP level in brain tissue of Huntington's disease transgenic mice, FEBS J 275 (2008) 4740-4755.

[44] F. Lopez-Rios, M. Sanchez-Arago, E. Garcia-Garcia, A.D. Ortega, J.R. Berrendero, F. Pozo-Rodriguez, A. Lopez-Encuentra, C. Ballestin, J.M. Cuezva, Loss of the mitochondrial bioenergetic capacity underlies the glucose avidity of carcinomas, Cancer Res 67 (2007) 9013-9017.

[45] K.M. Dipple, E.R. McCabe, Modifier genes convert "simple" Mendelian disorders to complex traits, Mol Genet Metab 71 (2000) 43-50.

ACCEPTED MANUSCRIPT

[46] K.M. Dipple, E.R. McCabe, Phenotypes of patients with "simple" Mendelian disorders are complex traits: thresholds, modifiers, and systems dynamics, Am J Hum Genet 66 (2000) 1729-1735.

[47] S. Dayal, E. Arning, T. Bottiglieri, R.H. Boger, C.D. Sigmund, F.M. Faraci, S.R. Lentz, Cerebral vascular dysfunction mediated by superoxide in hyperhomocysteinemic mice, Stroke 35 (2004) 1957-1962.

[48] F.M. Faraci, S.R. Lentz, Hyperhomocysteinemia, oxidative stress, and cerebral vascular dysfunction, Stroke 35 (2004) 345-347.

[49] D.J. Kim, J.M. Koh, O. Lee, N.J. Kim, Y.S. Lee, Y.S. Kim, J.Y. Park, K.U. Lee, G.S. Kim, Homocysteine enhances apoptosis in human bone marrow stromal cells, Bone 39 (2006) 582-590.

[50] J.M. Koh, Y.S. Lee, Y.S. Kim, D.J. Kim, H.H. Kim, J.Y. Park, K.U. Lee, G.S. Kim, Homocysteine enhances bone resorption by stimulation of osteoclast formation and activity through increased intracellular ROS generation, J Bone Miner Res 21 (2006) 1003-1011.

[51] C.F. Morel, J.P. Lerner-Ellis, D.S. Rosenblatt, Combined methylmalonic aciduria and homocystinuria (cblC): phenotype-genotype correlations and ethnic-specific observations, Mol Genet Metab 88 (2006) 315-321.

[52] A.C. Tsai, C.F. Morel, G. Scharer, M. Yang, J.P. Lerner-Ellis, D.S. Rosenblatt, J.A. Thomas, Late-onset combined homocystinuria and methylmalonic aciduria (cblC) and neuropsychiatric disturbance, Am J Med Genet A 143A (2007) 2430-2434.

[53] S.B. van der Meer, F. Poggi, M. Spada, J.P. Bonnefont, H. Ogier, P. Hubert, E. Depondt, D. Rapoport, D. Rabier, C. Charpentier, et al., Clinical outcome of

ACCEPTED MANUSCRIPT

long-term management of patients with vitamin B12- unresponsive methylmalonic acidemia, J Pediatr 125 (1994) 903-908.

[54] B. Merinero, B. Perez, C. Perez-Cerda, A. Rincon, L.R. Desviat, M.A. Martinez, P.R. Sala, M.J. Garcia, L. Aldamiz-Echevarria, J. Campos, V. Cornejo, M. Del Toro, A. Mahfoud, M. Martinez-Pardo, R. Parini, C. Pedron, L. Pena-Quintana, M. Perez, M. Pourfarzam, M. Ugarte, Methylmalonic acidaemia: examination of genotype and biochemical data in 32 patients belonging to mut, cblA or cblB complementation group, J Inherit Metab Dis 31 (2008) 55-66.

[55] A. Rincon, C. Aguado, L.R. Desviat, R. Sanchez-Alcudia, M. Ugarte, B. Perez, Propionic and Methylmalonic Acidemia: Antisense Therapeutics for Intronic Variations Causing Aberrantly Spliced Messenger RNA, Am J Hum Genet 81 (2007) 1262-1270.

ACCEPTE

ACCEPTED MANUSCRIPT

Table 1

Molecular and clinical description of patients with defects in Cbl metabolism analyzed in this work.

Patient No.	Gene affected (Complementation Group)	Genotype	Onset	Outcome	Reference[a] (P No.)
1	*MMAA (cblA)*	p.Q133X/p.Q133X	EO	A 18 y; DD	[54] (P20)
2	*MMAA (cblA)*	p.E199fs/p.E199fs	EO	A 12 y; DD; H	[54] (P25)
3	*MMAB (cblB)*	p.R186W/p.R186W	EO	D 10 d	[54] (P31)
4	*MMAB (cblB)*	p.I96T/p.S174fs	LO	D 4 y	[35] (P2)
5	*MMAB (cblB)*	p.I96T/p.S174fs		A	[35] (P3)
6	*MMACHC (cblC)*	p.R91KfsX14/ p.R91KfsX14	EO	D 5 m	[25] (P4)
7	*MMACHC (cblC)*	p.R91KfsX14/ p.R91KfsX14	EO	D 4 m	[25] (P5)
8	*MMACHC (cblC)*	p.R91KfsX14/ p.R91KfsX14	EO	NA	[25] (P6)
9	*MMACHC (cblC)*	p.R91KfsX14/ p.R91KfsX14	EO	A 8 y; DD; DVA; behavior problems	[25] (P7)
10	*MMACHC (cblC)*	p.R91KfsX14/ p.R91KfsX14	EO	D 6 m	[25] (P32)
11	*MMACHC (cblC)*	p.R91KfsX14/ p.R91KfsX14	EO	A 8 y; DD; DVA	[25] (P35)
12	*MMACHC (cblC)*	p.R91KfsX14/p.R153X	EO	D 3 y	[25] (P40)

ACCEPTED MANUSCRIPT

13	*MMACHC (cblC)*	p.R91KfsX14/c.81+2T > G	EO	A 24 m; DD; DVA	[25] (P41)
14	*MMACHC (cblC)*	p.R91KfsX14/p.R189S	LO	A 18 y; asymptomatic	[25] (P43)
15	*MMACHC (cblC)*	p.R91KfsX14/p.M1L	EO	A 5 y; DD; DVA; S	[25] (P44)
16	*MMACHC (cblC)*	p.R91KfsX14/p.R161X	EO	A 8 y; DD; DVA	[25] (P47)
17	*MUT (mut^0)*	p.V583fs/c.1957-891C > A	EO	D 5 y	[55]
18	*MTRR (cblE)*	p.V56M/p.V56M	EO	A 25 m, DD	Not reported
19	*CBS*	p.T191M/ p.T191M	NA	NA	Not reported

[a]P No., patient number in each reference is indicated.
EO, early onset (less than one year of age); LO, late onset (older than one year of age); A, alive; D, died; DD, developmental delay; DVA, decreased visual acuity; H, hypotonia; S, seizures; NA, not available; y, year; m, month; d, day. Patient 4 and 5 are siblings; P4 presented a fatal crisis and suddenly died at 4 years of age; P5 is clinically normal.

ACCEPTED MANUSCRIPT

ACCEPTED MANUSCRIPT

Table 2

Fold-change profile of apoptotic genes in fibroblasts from patients with *cblB* and *cblC* disorders.

GeneBank Accession	Description	Gene symbol	*cblB*-fold change	*cblC*-fold change
Pro-apoptotic genes				
TNF ligand family				
NM_000595	Lymphotoxin alpha (TNF superfamily member 1)	LTA	1.75	2.1
NM_000594	Tumor necrosis factor (TNF superfamily member 2)	TNF	1.4	1.9
NM_003810	Tumor necrosis factor (ligand) superfamily member 10	TNFSF10	1.7	1.54
TNF receptor family				
NM_001250	Tumor necrosis factor receptor superfamily, member 5	TNFRSF5	0.37	1.3
NM_001065	Tumor necrosis factor receptor superfamily, member 1A	TNFRSF1A	0.61	1.55
NM_003790	Tumor necrosis factor receptor superfamily, member 25	TNFRSF25	0.48	5.35
NM_003844	Tumor necrosis factor receptor superfamily, member 10A	TNFRSF10A	0.77	1.79
NM_003842	Tumor necrosis factor receptor superfamily, member 10B	TNFRSF10B	0.47	0.8

ACCEPTED MANUSCRIPT

NM_014452	Tumor necrosis factor receptor superfamily, member 21	TNFRSF21	0.4	1.38
NM_001242	CD27 molecule	CD27	1.67	2.1
NM_001561	Tumor necrosis factor receptor superfamily, member 9	TNFRSF9	1.44	2.12
NM_002342	Lymphotoxin beta receptor (TNFR superfamily member 3)	LTBR	1.76	1.74
Bcl-2 family				
NM_003806	Harakiri, BCL2 interacting protein	HRK	17.6	7.1
NM_001197	BCL2-interacting killer (apoptosis inducing)	BIK	1.4	1.8
NM_004324	BCL2-associated X protein	BAX	0.9	1.9
NM_014739	BCL-2 associated transcription factor 1	BCLAF1	0.6	0.56
Caspase family				
NM_033292	Caspase 1, apoptosis-related cysteine peptidase	CASP1	1.79	1.25
NM_004346	Caspase 3, apoptosis-related cysteine peptidase	CASP3	0.78	0.52
NM_001227	Caspase 7, apoptosis-related cysteine peptidase	CASP7	0.8	1.51
NM_001229	Caspase 9, apoptosis-related cysteine peptidase	CASP9	1.61	1.3
NM_001230	Caspase 10, apoptosis-related cysteine peptidase	CASP10	1.32	1.59

ACCEPTED MANUSCRIPT

CARD family				
NM_006092	Nucleotide-binding oligomerization domain containg 1	NOD1	1.74	2.01
NM_001160	Apoptotic peptidase activating factor 1	APAF1	1.64	1.68
NM_014959	Caspase recruitment domain family, member 8	CARD8	0.4	0.93
Death domain				
NM_004938	Death-associated protein kinase 1	DAPK1	0.5	1.1
Death effector domain				
NM_003824	Fas (TNFRSF6)-associated via death domain	FADD	0.42	0.8
CIDE domain family				
NM_001279	Cell death-inducing DFFA-like effector a	CIDEA	1.4	1.7
NM_014430	Cell death-inducing DFFA-like effector b	CIDEB	0.9	1.93
p53 family				
NM_005426	Tumor protein p53 binding protein, 2	TP53BP2	0.4	0.74
NM_000546	Tumor protein p53 (Li-Fraumeni syndrome)	TP53	0.4	0.49
Antiapoptotic genes				

ACCEPTED MANUSCRIPT

Bcl-2 family				
NM_000633	B-cell CLL/lymphoma 2	BCL2	0.94	1.7
NM_021960	Myeloid cell leucemia sequence 1 (BLC2-related)	MCL1	1.6	1.86
NM_004323	BCL2-associated athanogene	BAG1	2.12	1.9
NM_004049	BCL2-related proteína A1	BCL2A1	2.01	1.82
NM_138578	BCL2-like 1	BCL2L1	0.9	1.59
IAP family				
NM_004536	NLR family, apoptosis inhibitory protein	NAIP	0.7	2.08
NM_001165	Baculoviral IAP repeat-containing 3	BIRC3	0.68	1.51
NM_001167	Baculoviral IAP repeat-containing 4	BIRC4	0.75	1.54
TRAF family				
NM_021138	TNF receptor-associated factor 2	TRAF2	0.39	2.1
NM_003300	TNF receptor-associated factor 3	TRAF3	0.57	1.81
NM_004295	TNF receptor-associated factor 4	TRAF4	0.53	2.18
CARD family				

ACCEPTED MANUSCRIPT

ACCEPTED MANUSCRIPT

NM_003946	Nucleolar protein 3 (apoptosis repressor with CARD domain)	NOL3	1.75	1.8
Death effector domain				
NM_003879	CASP8 and FADD-like apoptosis regulator	CFLAR	0.54	1.61
Other genes				
NM_005163	V-akt murine thymoma viral oncogene homolog 1	AKT1	0.57	1.77
NM_004333	V-raf murine sarcoma viral oncogene homolog B1	BRAF	1.2	1.79
NM_016561	Bifunctional apoptosis regulator	BFAR	0.6	0.52

ACCEPTED MANUSCRIPT

ACCEPTED MANUSCRIPT

Table 3

Gene expression categories in *cblB* and *cblC* cell lines.

	cblB	***cblC***
Pro-apoptotic genes		
Overexpressed genes	HRK, LTA, CD27, LTBR, NOD1, TNFSF10, CASP9, CASP1, APAF1	HRK, LTA, CD27, LTBR, NOD1, CASP10, TNFSF10, APAF1, TNFRSF1A, TNFRSF25, CIDEB, BAX, CASP7, TNFRSF10A, TNF, BIK, TNFRSF9, CIDEA
Under-expressed genes	TP53BP2, TP53, TNFRSF1A, TNFRSF25, CARD8, TNFRSF10B, FADD, DAPK1, TNFRSF5, TNFRSF21, BCLAF1	TP53, BCLAF1, CASP3
Antiapoptotic genes		
Overexpressed genes	MCL1, BAG1, BCL2A1, NOL3	MCL1, BAG1, BCL2A1, NOL3, TRAF4, TRAF2, TRAF3, AKT1, NAIP, BRAF, BIRC3, BIRC4, BCL2, BCL2L1, CFLAR
Under-expressed genes	BFAR, TRAF4, TRAF2, TRAF3, AKT1, CFLAR	BFAR

ACCEPTED MANUSCRIPT

Table 4

Gene expression response to retroviral infection in *cblC* and *cblB* cell lines which express MMACHC protein.

Patients	Down-regulated Genes	Up-regulated Genes
P6 (*cblC*)	BAG3, BAK1, BAX, GADD45A, LTA, TNF, TNFRSF10B, TRAF2	CARD8
P7 (*cblC*)	AKT1, APAF1, BCL2A1, BAK1, BIRC2, BIRC3, BIRC4, CARD6, CASP10, CFLAR, CIDEB, IGF1R, DFFA, FADD, NOD1, NOL3, TNFSF10, TNFRSF10B, TNFRSF11B	BNIP2
P4 (*cblB*)	BAX, BCL2L1, CFLAR, CASP7	CARD8

ACCEPTED MANUSCRIPT

ACCEPTED MANUSCRIPT

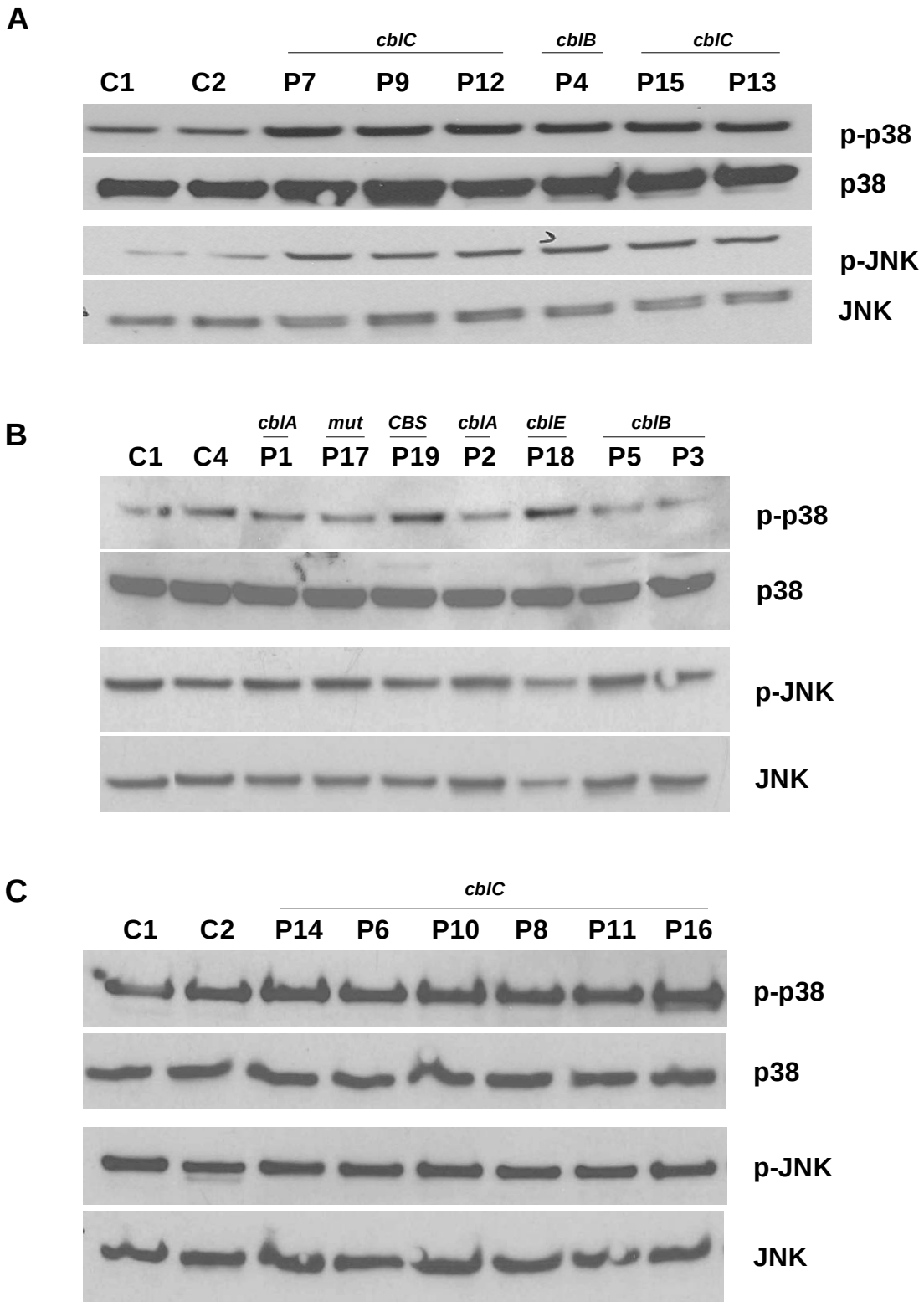

Figure 1

Figure 1. Analysis of phosphorylated p38 and JNK stress-activated protein kinases expression in patients´ fibroblasts. (A, B and C) Equal amounts of controls (GM09503

ACCEPTED MANUSCRIPT

(C1), GM08333 (C2) and GM08680 (C4)) and patients´ samples (Table 1) were loaded (40 µg of total cell lysates) and subjected to immunoblotting with anti-phosphorylated p38 and anti-phosphorylated JNK antibodies. The stripped blots were reprobed with total anti-p38 and total anti-JNK antibodies as evidence of the equivalent amounts of protein loaded in each lane. The results in each case are representative of at least three independent experiments. Patients along with the complementation groups they belong to are depicted in the upper panels. C: control; P: patient.

ACCEPTED MAN

ACCEPTED MANUSCRIPT

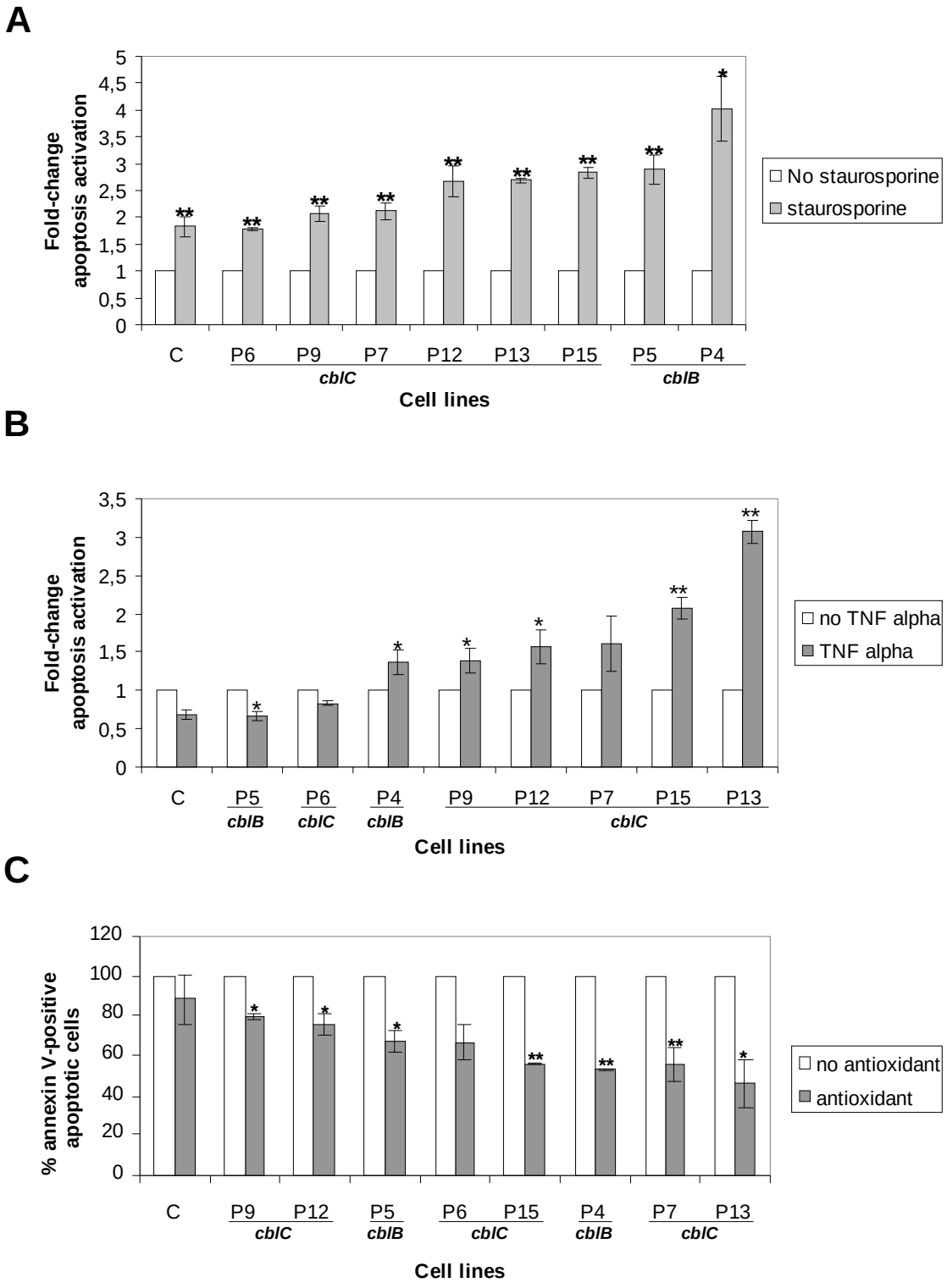

Figure 2

Figure 2. Detection of annexin V-apoptosis in control and patients´ fibroblasts by flow cytometry. (A) Staurosporine treatment. Cells were incubated in 2 µM of staurosporine for 1 h. (B) TNF-α and CHX treatment. Fibroblasts were incubated with 20 ng/ml of

ACCEPTED MANUSCRIPT

TNF-α and 25 µg/ml of CHX for 20 h. (C) Antioxidant treatment. Cell lines were incubated with 20 mM of Tiron® for 20 h. Results are expressed as apoptotic positive cells in stimulus-treated fibroblasts relative to the corresponding untreated cells. Data represent mean ± SD of two independent experiments, each one performed by triplicated (*P< 0.05; **P<0.01). Patients along with the complementation groups they belong to are depicted in the figure. C: control; P: patient.

Supplementary Figure 1. Densitometric and statistical analysis of stress-kinases activation in patients´ fibroblasts. (A) p38 fold-change activation. (B) JNK fold-change activation. Protein quantification was performed by laser densitometry. The ratios between phosphorylated/total kinase forms for each cell line were calculated to determine the activation fold-change relative to controls. Data represent mean ± SD of three independent experiments (*P< 0.05; **P<0.01). Patients along with the complementation groups they belong to are depicted in the figure. C: control; P: patient.

Supplementary Figure 2. Analysis of NOL-3 (A) and BCL-2 (B) protein expression in patients´ fibroblasts. Equal amounts of controls and patients´ samples were loaded (40 µg (A) and 200 µg (B) of whole-cell lysates) and subjected to Western blotting using anti-NOL3 and anti-BCL-2 antibodies. The results in each case are representative of three independent experiments. The stripped blots were reprobed with anti-α-tubulin antibody as evidence of the equivalent amounts of protein loaded in each lane. Patients along with the complementation groups they belong to are depicted in the upper panels. C: control; P: patient.